The effect of the input energy on the SOA gain with non-uniform biasing

A. Abd El Aziz[1], W. P. Ng[1], Z. Ghassemlooy[1], Moustafa Aly[2], R. Ngah[3], M. F. Chiang[1]
[1]*Optical Communications Research Group, NCRLab Northumbria University, Newcastle upon Tyne, UK*
Tel: (+44)1912273841, e-mail: ahmed.shalaby@northumbria.ac.uk
[2]*Arab Academy for Science and Technology, Alexandria, Egypt*
[3]*Universiti Teknologi, Malaysia*

This paper investigates the effect of input optical pulse energy on the total gain of the semiconductor optical amplifier (SOA) injected with a non-uniform bias current. For ultra-high data rate applications it is essential that the SOA has a fast gain recovery response, thus resulting in maximum SOA gain and reduced gain standard deviation. SOA with higher gain standard deviation will reduce the overall gain of the output optical pulses. Therefore in this paper, non-uniform biasing techniques are adopted in order to accelerate the gain recovery while minimizing the gain standard deviation for high-speed optical applications. The theoretical SOA operation principle is demonstrated using segmentized model with the complete rate and propagation equations. The gain responses of the SOA due to uniform and non-uniform biasing techniques are analyzed. Different recovery rates are investigated using the non-uniform biasing to optimize the gain. This paper will present the effect of the input pulse energy on the output gain and the gain standard deviation employing different bias current techniques at speed up to 40 Gbps.

1. Introduction

For many years, there has been a desire to realize all-optical computers using digital optical components. The requirements are not for massive processing, but rather the possibility of simple optical processing at bit rates close to or beyond the bandwidth of presently available electronics devices (i.e. 40 Gbps and above). Ultrafast photonic core networks will increasingly rely on all-optical signal processing to avoid the bottleneck imposed by the electronic and optoelectronic devices [1]. In all-optical signal processing, switching and routing one component is considered as the key building block, which is the semiconductor optical amplifier (SOA). SOAs can be used as an amplifier or as a switch. The latter is based on exploiting SOA's fast nonlinear characteristics, which has be adopted in a number of applications including optical signal processing, clock recovery, ultra fast optical time multiplexing/demultiplexing, pulse shaping, all-optical switching, dispersion compensation and wavelength conversion in wavelength division multiplexing to name a few [2]**.** Ultrafast all-optical switches based on the SOA, such as Mach-Zehnder Interferometers (MZIs) are the most promising candidates for the realization of all-optical switching and processing applications compared to other all-optical switches, such as ultrafast-nonlinear interferometers (UNIs) and Terahertz Optical Asymmetric Demultiplexers (TOADs). This is because of their small size, a low switching energy, high stability, high integration potential and their fast, and strong nonlinearity characteristics [3].

The SOA performance is measured, to a great extent, by their gain recovery response. For high-speed applications, the SOA must have a fast gain recovery time to avoid system penalties arising from bit pattern dependencies [4]. The gain recovery of the conventional SOAs is limited by the long carrier-recovery time, and can only be moderately improved by increasing the injected bias current, the device length or by changing the pulse width (input energy) of the input signal [5]. Several research groups have reported theoretical and experimental results on externally injected SOAs, where an assist light is applied at the transparency point of the SOA. Thus allowing high speed operation at a current identical to that of a conventional SOA [6]. Meanwhile applying a continuous wave (CW) holding beam can maintain the separation of the quasi-Fermi levels and speed-up the SOA recovery rate. However, the drawback with this solution is the large reduction in the available gain as the CW injection is in the gain region as reported in [7].

In this paper, non-uniform bias current is injected into the SOA in order to achieve a linear output gain compared to the uniform biasing. To the best of the author's knowledge, no work has been reported on the SOA with non-uniform bias current. The SOA gain response and the corresponding output power are demonstrated for uniform, sawtooth and triangular biasing schemes. The impacts of both uniform and non-uniform biasing on the average gain deviation are investigated at the router speed up to 40 Gbps. The paper also simulates the effect of the input optical pulse energy and different average bias current on the gain standard deviation. The following section will show the SOA principle of operation. The mathematical analysis of the total gain and the change of the carrier density in terms of the rate equations are shown in section 3. Section 4 presents the proposed segmentized model. The SOA response to the uniform biasing is presented in section 5 while section 6 shows the results and the environment required to achieve an improvement in the output gain uniformity for non-uniform biasing. The final section concludes the findings of the investigation.

2. SOA Principle of Operation

The SOA consists of a fixed waveguide between a p-n junction through which the propagating signal wave is bounded to the active region. Gain occurs when an external direct current (DC) is applied to supply the energy source to the active region, which results in the formation of electrons in the conduction band from the valence band [8]. When a short input optical pulse is launched into the SOA, stimulation emission will take place resulting in signal amplification [9]. At the same time the excited electrons in the conduction band (i.e. the carrier density) will decrease due to the interaction with input pulse. Hence this reduction will result in a decrease in the SOA gain because the gain is proportional to the carrier population [10]. The carrier non-equilibrium is governed mainly by the spectral hole burning effect [9]. The distribution recovers to equilibrium by carrier-carrier scattering. Instantaneous mechanisms such as two-photon absorption [6] and the optical Kerr effects [10] will then influence on the SOA response. After few picoseconds, a quasi-equilibrium distribution will occur due to the carrier temperature relaxation process and then the carrier density will be recovered [8]. The gain recovery is limited by the carriers' lifetime.

3. Theoretical Model

A numerical model was developed to analyze the bias current and its effect on the gain spectrum. The model is based on position-dependent rate equations for the carrier density and the optical propagation equation in the forward-propagating direction for injected input signals. Therefore, the model accounts for a non-uniform carrier distribution. The complete rate equations in small segments in an SOA are iteratively calculated with third order gain coefficients.

3.1 Rate equations:

When light is injected into the SOA, changes occur in the carrier and photon densities within the active region of the SOA. These changes can be described using the rate equations [11]. The dynamic equation for the change in the carrier density within the active region of the device is given by:

$$\frac{dN}{dt} = \frac{I}{q \cdot V} - (A \cdot N + B \cdot N^2 + C \cdot N^3) - \frac{\Gamma \cdot g \cdot P_{av} \cdot L}{V \cdot h \cdot f}, \quad (1)$$

where I is the DC current injected to the SOA, q is the electron charge and V is the active volume of the SOA, Γ is the confinement factor, P_{av} the average output power, L is the SOA length, h is the Plank constant and f is the light frequency. A is the surface and defect recombination coefficient while B and C are the radiative and Auger recombination coefficients, respectively. The gain medium of the amplifier is described by the material gain coefficient, g (per unit length), which is dependent on the carrier density N and the signal wavelength λ and is given by:

$$g = \frac{a_1(N - N_O) - a_2(\lambda - \lambda_N)^2 + a_3(\lambda - \lambda_N)^3}{1 + \varepsilon \cdot P_{av}}, \quad (2)$$

where a_2 and a_3 are empirically determined constants that characterize the width and asymmetry of the gain profile, respectively. a_1 is the differential gain parameter, N_o is the carrier density at transparency point and ε is the gain compression factor. The corresponding peak gain wavelength is given by:

$$\lambda_N = \lambda_O - a_4(N - N_O). \quad (3)$$

where λ_o is the peak gain wavelength at transparency and a_4 is the empirical constant that shows the shift of the gain peak.

3.2 Propagation equation

Assuming insignificant reflectivity at the end facets, the propagation equation for the forward light is given by [11]:

$$\frac{dP_{in}}{dz} = (\Gamma \cdot g - \alpha_s)P_{in}, \quad (4)$$

where P_{in} is the input signal power and α_s is the internal waveguide scattering loss.

4. Amplification Process and Segmentized Model

The segmentation model in this paper uses the rate equations in Section 3 to investigate the SOA gain and the power of the emerging output signal in Matlab™. In the segmentization method, the SOA is divided into five equal segments of length $l = L/5$ each, where l is the segment length, and the carrier density is assumed to be constant within each segment. However, the carrier density and the signal power changes from segment-to-segment depending on input power and the carrier

density of the previous segment. The reason for five segments is to investigate the change in the carrier density and the signal gain along the SOA. Each segment contain a full pulse with a width of l/v_g (i.e. 1.167 ps), where v_g is the group velocity of the signal within the active region of the waveguide [8]. To calculate the segment total gain and its carrier density, the SOA length L is replaced with l in all the equations given in section 3. The physical SOA parameters used are given in the Table presented in [12].

5. Uniform Biasing

In this section, the bias current applied to the SOA is uniform with I = 150 mA. With bias current applied to the SOA, the gain increases rapidly until it reaches its maximum equilibrium value. This process is shown in Fig. 1 for t < 1 ns. The reason for such response is that a large number of electrons located in the valence band will gain enough energy, due to the biasing, to overcome the energy gap. Therefore, these electrons will increase the number of excited electrons in the conduction band (i.e. carrier density), thus resulting in increased total gain of the SOA. Figure 1 also shows the normalized gain response of the SOA when injected with a single (doted) input pulse and multiple (solid) short input pulses. Applying 1 fJ input pulse to the active region of the SOA will result in an interaction between the input pulse and the excited electrons in the conduction band (i.e. stimulated emission), thus leading to a decrease in the carrier density. Due to the dependence of the gain on the carrier density shown in (2), a sudden depletion will occur in the total gain of the SOA. Following exit of the input pulse from the waveguide, the SOA gain shows a slow recovery (hundreds of picoseconds) to its equilibrium value [13] (see Fig. 2 doted). The solid line in Fig. 1 shows the SOA gain response to a train of input pulses with the same input energy and a data rate of 10 Gbps.

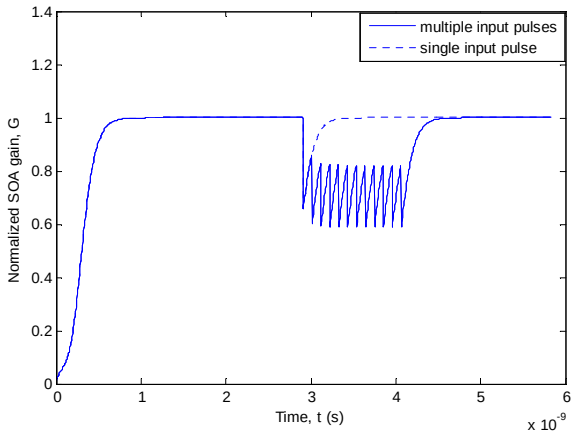

Figure 1: Normalized SOA gain response to single (doted) and multiple (solid) input pulses.

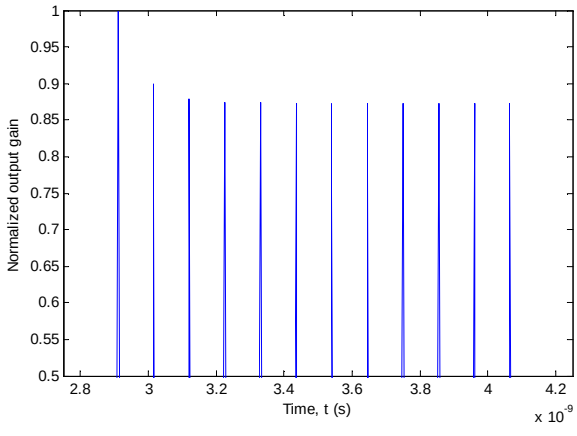

Figure 2: Normalized output gain achieved by successive input pulses.

Prior to applying the first pulse to the SOA, the third term of equation 1 is equal to zero as the input energy is zero. Therefore, the change of the carrier density shown in the equation can be neglected. This is because the first and second terms of the rate equation 1 are constants. When the first pulse is launched to the SOA, the third term in (1) becomes the dominant. The presence of the third term results in a rapid depletion in the carrier density, thus causing dN/dt to have a higher negative value. Consequently, a gap between the first and second terms of the (1) occurs when the pulse exits the SOA (i.e. 3rd term is zero). Therefore, dN/dt will have a positive value

and the carrier density will start to increase (i.e. SOA gain recovery). Due to the slow gain recovery of the SOA, when the next pulse enters the SOA, it will result in higher total gain depletion. This process will continue until the last pulse exits the SOA.

The output gain achieved by the input pulses is proportional to the drop in gain of the SOA. Figure 2 illustrates the normalized output gain as a function of the input pulse train, showing a non-flat (large standard deviation) gain response. In order to minimize the gain fluctuation (i.e. minimize the gain standard deviation), it is important to increase the recovery rate of the gain. To that end, there is a need to increase the gap between both the first and second terms of (1) (following pulse exits from the SOA) to speed-up the gain recovery rate and hence, decrease the gain standard deviation. This can not be obtained in the case of the uniform biasing as the first term of the rate equation is always constant. Therefore, non-uniform biasing techniques are proposed in this paper in order to control the rate of change of the carrier density.

6. Non-uniform Biasing

This section proposes triangular and sawtooth biasing techniques to increase the rate of carrier density recovery. The average bias current applied to the SOA in both cases is 150 mA (same as uniform biasing) to maintain the same power used in all cases. Figure 3 displays both the triangular and sawtooth bias current applied to the SOA with both plots having the same positive slope to maintain the rising rate. For input pluse train with a period of T = 100 ps, the triangular bias current can be expressed by:

$$I = \begin{cases} m_1 t + C_1 & for \quad 0 \le t \le T/2 \\ m_2 t + C_2 & for \quad T/2 \le t \le T \end{cases}, \tag{5}$$

where m_1 and m_2 are the slopes of the triangular signal with values 30.257 and -30.257 mA/ns, respectively. C_1 and C_2 are 70.55 mA and 388.25 mA, respectively. On the other hand, the sawtooth bias current is defined by:

$$I = m_1 t \,. \tag{6}$$

In Fig. 4, the normalized SOA gain response to the triangular bias current is plotted. From Fig. 1, the fluctuation of the gain profile that occurs due to the triangular bias current shape is observed. The impact of applying input pulse train with the same characteristics as in the uniform bias current on the SOA gain is shown in Fig. 4 (circled). Figure 5 depicts the corresponding pulses output gain showing a reduced gain compared to the uniform biasing due to the lower carrier density. Nevertheless, the fluctuations of output gain are lower (improved uniformity). Same input pulse stream with same characteristics are also applied to the SOA with sawtooth biasing. The normalized SOA gain and the corresponding output gain achieved by the input pulses due to sawtooth bias current shape are shown in Figs. 6 and 7, respectively. The oscillation observed in the SOA gain profile, see Fig. 6, is due to the larger range of the bias current (0 to 300 mA). Accordingly, lower output gain is achieved by the input pulses with lower average gain fluctuations as presented in Fig. 7.

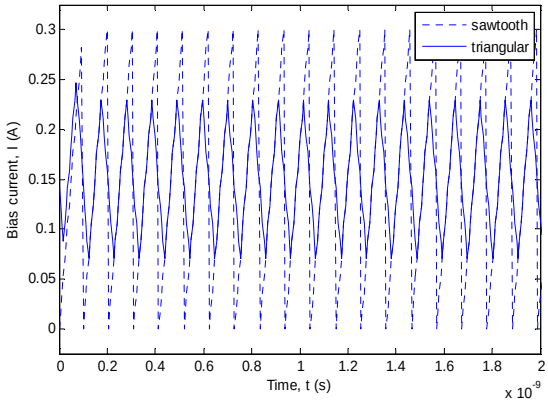

Figure 3: Sawtooth (doted) and triangular (solid) bias currents.

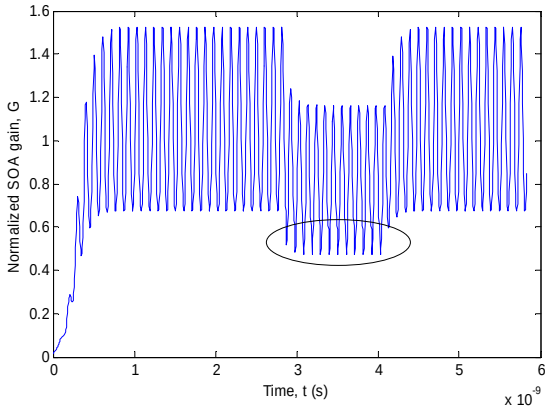

Figure 4: Normalized SOA gain response to multiple of input pulses using triangular bias current.

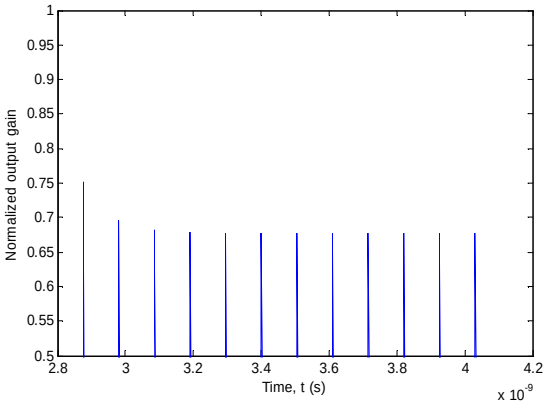

Figure 5: Normalized output gain achieved by successive input pulses using triangular bias current as a ratio of uniform bias current

A comparison between all the proposed biasing techniques is shown in Fig. 8 for different input signal energies at different data rates of 10, 20 and 40 Gbps. Figure 8 shows that the gain standard deviation is lower for the non-uniform biasing techniques, especially at 10 and 20 Gbps data rates. At 1 fJ and at a data rate of 10 Gbps the non-uniform biasing techniques showed improved gain standard deviation improvement of 3.25 dB and 2.4 dB for the sawtooth and triangular biasing schemes, respectively compared to the uniform biasing. Meanwhile at 20 Gbps, the improvement are 0.51 dB and 0.4 dB for sawtooth and triangular, respectively. At the speed of 40 Gbps minimum improvement is achieved. This is because high speed input pulse stream restricts the full recovery of the SOA gain in contrast to lower data rates. Moreover, at higher rates (particularly at 40 Gbps), the output gain has a higher standard deviation due to the reduced pulse period. As expected, the sawtooth bias current shows a lower gain standard deviation (better gain uniformity) than the triangular biasing in all cases. It is also shown that the gain standard deviation increases with the input signal energy which results from the larger value of the third term in the rate equation 1.

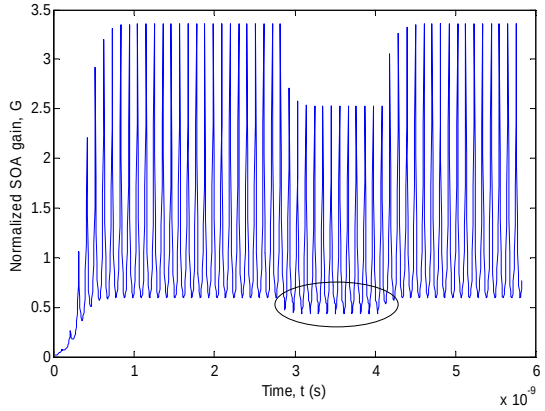

Figure 6: Normalized SOA gain response to multiple of input pulses using sawtooth bias current.

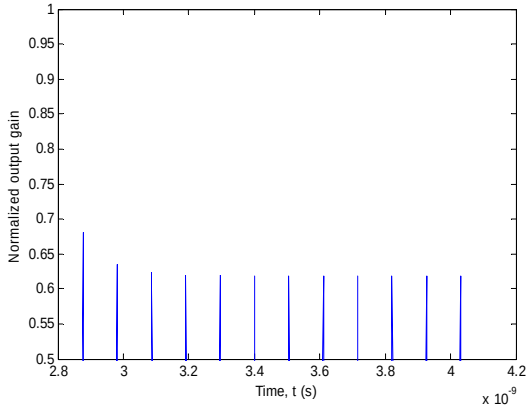

Figure 7: Normalized output gain achieved by successive input pulses using sawtooth bias current as a ratio of uniform bias current.

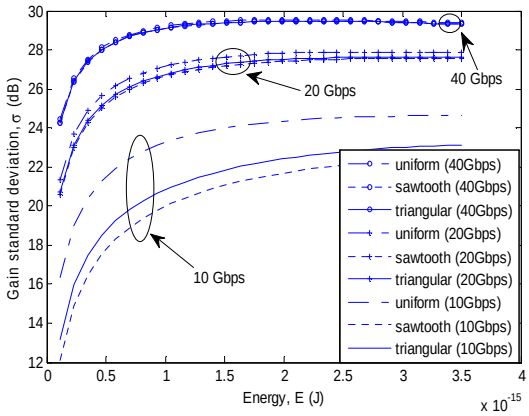

Figure 8: Gain standard deviation against the input signal energy for uniform (dot-dashed), sawtooth (doted) and triangular (solid) biasing for a range of data rates.

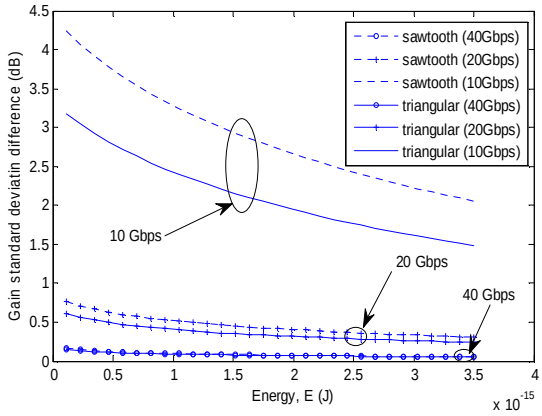

Figure 9: Gain standard deviation improvement of sawtooth (doted) and triangular (solid) over uniform biasing to the input signal energy for range of data rates.

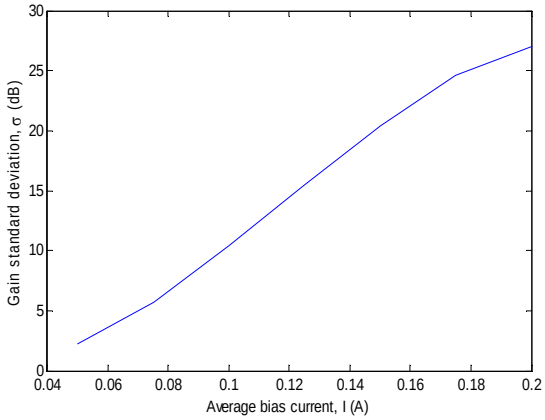

Figure 10: Gain standard deviation against the average sawtooth bias current for 1 fJ input signal energy.

The advantage of using non-uniform techniques over uniform biasing is more evident in Fig. 9. The figure illustrates the improvement of the gain standard deviation for uniform and non-uniform (triangular and sawtooth) bias currents. Figure 10 depicts the gain standard deviation against a range of different average sawtooth bias current for input pulses with 1 fJ energy. The sawtooth bias current technique shows the best response

because it achieves the lowest gain standard deviation value (best gain uniformity), see Fig. 9. In Fig. 10 the gain standard deviation increases as the average bias current increases. The reason for such response is because of higher depletion of the carrier density at the presence of the third term in (1). Therefore it is important to minimize the average bias current in order to reduce the gain standard deviation and yet at the same time large enough to accelerate the carrier density recovery.

7. Conclusion

This paper proposed non-uniform techniques to bias the SOA. The paper has simulated the total gain response of a segmentized SOA model. Both the SOA and the output gain for uniform and non-uniform biasing schemes were analyzed. This paper has presented the investigation of applying triangular and sawtooth biasing techniques in order to optimize the gain standard deviation for data rates of 10, 20 and 40 Gbps. The results showed an enhancement to the gain uniformity achieved using non-uniform biasing; especially the sawtooth shaped bias current. The impact of the input pulse energy on the gain standard deviation and the output gain were also investigated and compared for uniform and non-uniform biasing techniques. The impact of the average bias current used on the gain uniformity is presented.

References

[1] K. Stubkjaer, "Semiconductor optical amplifier-based all-optical gates for high-speed optical processing," *IEEE Journal on Selected Topics in Quantum Electronics,* vol. 6, pp. 1428-1435, 2000.

[2] E. Tangdiongga, Y. Liu, H. Waardt, G. Khoe, A. Koonen, and H. Dorren, "All-optical demultiplexing of 640 to 40 Gbits/s using filtered chirp of a semiconductor optical amplifier," *Optics Letters,* vol. 32, pp. 835-837, 2007.

[3] J. Moerk, M. Nielsen, and T. Berg, "The dynamics of semiconductor optical amplifiers-modeling and applications," *Optics and Photonics News,* vol. 14, pp. 42-48, 2003.

[4] B. Leuthold, B. Mikkelsen, G. Raybon, C. H. Joyner, J. L. Pleumeekers, B. I. Miller, K. Dreyer, and R. E. Behringer, "All-optical wavelength conversion between 10 and 100 Gb/s with SOA delayed-interference configuration," *Optical and Quantum Electronics,* vol. 33, pp. 939-952, 2001.

[5] F. Ginovart and J. C. Simon, "Semiconductor optical amplifier length effects on gain dynamics," *Journal of Physics D: Applied Physics,* vol. 36, pp. 1473-1476, 2003.

[6] H. Ju, A. Uskov, R. Notzel, Z. Li, J. Vazquez, D. Lenstra, G. Khoe, and H. Dorren, "Effects of two-photon absorption on carrier dynamics in Quantum-dot optical amplifiers," *applied physics B. lasers and optics,* vol. 82, pp. 615-620, 2006.

[7] W. Hong, D. Huang, and G. Zhu, "Switching window of an SOA-loop-mirror with SOA sped-up by a CW assist light at transparency wavelength," *Optics Communications,* vol. 238, pp. 151-156, 2004.

[8] H. Le Minh, "All-optical router with PPM header processing high speed photonic packet switching networks," Northumbria University, 2007.

[9] L. Guo and M. Connelly, "All-optical AND gate with improved extinction ratio using signal induced nonlinearities in a bulk semiconductor optical amplifier," *optics Express,* vol. 14, pp. 2938-2943, 2006.

[10] G. Agrawal, *Nonlinear fiber optics*, 2 ed. San Diego, USA: Academic Press, 1995.

[11] H. Wang, J. Wu, and J. Lin, "Studies on the material transparent light in semiconductor optical amplifiers," *Journal of Optics A:Pure and Applied Optics,* vol. 7, pp. 479-492, 2005.

[12] A. Abd El Aziz, W. P. Ng, Z. Ghassemlooy, M. H. Aly, R. Ngah, and M. F. Chiang, "Characterization of the Semiconductor Optical Amplifier for Amplification and Photonic Switching Employing the Segmentation Model," *International Conference on Transparent Optical Networks ''Mediterranean Winter'' 2008* pp. Fr1A.1 (1-6), 11-13 December 2008.

[13] J. L. Pleumeekers, M. Kauer, K. Dreyer, C. Burrus, A. G. Dentai, S. Shunk, J. leuthold, and C. H. Joyner, "Acceleration of gain recovery in semiconductor optical amplifiers by optical injection near transparency wavelength," *IEEE photonics technology letters,* vol. 14, pp. 12-14, 2002.